S0375-9601(05)01325-3/SCO AID:14863 Vol.●●●(●●●)
PLA:m3 v 1.46 Prn:13/09/2005; 8:26

pla14863

[DTD5] P.1 (1-11)
by:PS p. 1

Available online at www.sciencedirect.com
SCIENCE DIRECT®

Physics Letters A ●●● (●●●●) ●●●–●●●

PHYSICS LETTERS A

www.elsevier.com/locate/pla

Scaling behavior of high resolution temporal rainfall: New insights from a wavelet-based cumulant analysis

Venugopal V. [a,*], Stéphane G. Roux [b], Efi Foufoula-Georgiou [a], Alain Arnéodo [b]

[a] *St. Anthony Falls Laboratory, University of Minnesota, Mississippi River at 3rd Avenue SE, Minneapolis, MN 55414, USA*
[b] *Laboratoire de Physique, Ecole Normale Superieure de Lyon, 46 Allée d'Italie, 69364 Lyon cédex 07, France*

Received 24 May 2005; received in revised form 23 August 2005; accepted 23 August 2005

Communicated by F. Porcelli

Abstract

We revisit the multifractal analysis of high resolution temporal rainfall using the wavelet transform modulus maxima (WTMM) method. Specifically, we employ a cumulant analysis of the logarithm of the WTMM coefficients to estimate the scaling exponent spectrum $\tau(q)$ and the spectrum of singularities $D(h)$. We document that rainfall intensity fluctuations exhibit multifractality from scales of the order of 4–5 minutes up to the storm-pulse duration of 1–2 hours. We also establish long-range dependence consistent with that of a multiplicative cascade.

Keywords: Wavelets; Scaling; Precipitation; Multifractal; Multiplicative cascades

1. Introduction

High resolution temporal rainfall (sampling interval of the order of seconds to minutes) has been studied by many researchers for the purpose of extracting its scaling characteristics (e.g., [1–13]; among others). Most of these studies have used spectral analysis or traditional multifractal analysis based on computing higher order moments of the data or their fluctuations (e.g., box counting or structure function analysis) to estimate the scaling exponent function $\tau(q)$ and, via a Legendre transform, the singularity spectrum $D(h)$. In this Letter, motivated by the most recent developments in multifractal analysis of turbulence signals (e.g., [14, 15]), we re-examine the scaling structure of high resolution temporal rainfall using wavelet-based estimators (see also [16] for application to cloud structure). Specifically, we use a one- and two-point cumulant analysis of the WTMM magnitude to infer the nature of multifractality and estimate the scaling exponents of high resolution temporal rainfall.

It is noted that the typical multifractal analysis consists of estimating the $\tau(q)$ curve (see next section for

* Corresponding author.
E-mail address: venu@msi.umn.edu (Venugopal V.).

0375-9601/$ – see front matter
doi:10.1016/j.physleta.2005.08.064

S0375-9601(05)01325-3/SCO AID:14863 Vol.●●●(●●●)
PLA:m3 v 1.46 Prn:13/09/2005; 8:26

definitions) by taking moments of the data (or their increments) of increasingly higher order q, plotting log-moment versus log-scale, and estimating the slopes of these log–log linear curves. This is typically done for several moments including fractional moments, e.g., $q = 0.2$ up to 5.0 (or higher). The slopes of these lines are then plotted versus order of moment and a nonlinear curve is fitted to that plot to estimate the $\tau(q)$ curve. It is easy to see that one has to resort to higher order moments to capture the nonlinearity of the $\tau(q)$ curve (note that a linear approximation would imply the presence of monofractality in the data). Taking higher order moments of small data sets (say of the order of a few hundred points) is problematic and renders the estimation of the $\tau(q)$ curve unreliable. Once the $\tau(q)$ curve is estimated, a Legendre transform is applied to estimate the $D(h)$ curve, i.e., $D(h) = \min_q[qh - \tau(q)]$. Here it is noted that by using positive order moments only ($q > 0$), one has access to the increasing part of the $D(h)$ spectrum only (recall that derivatives of the $D(h)$ curve are the moment orders q, i.e., $dD(h)/dh = q$; see Fig. 1). This makes it hard to accurately define the whole spectrum of singularities and especially the maximum Hölder exponent $h_{\max}$. It is also noted that taking negative moments ($q < 0$) is not always feasible. For example, when working with the increments of the data, i.e., when using the so-called structure function approach, the probability density function (PDF) of the increments is centered close to zero and taking negative moments creates divergences as values very close to zero are raised to negative powers [17]. Note also

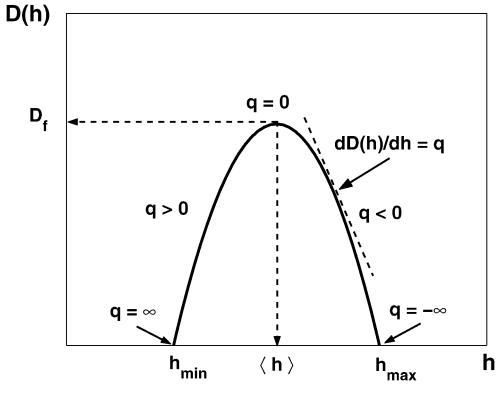

Fig. 1. Generic shape of the $D(h)$ singularity spectrum considered as the Legendre transform of $\tau(q)$.

that the structure function method fails to provide estimate of the fractal dimension $D_f = -\tau(q = 0)$ of the support of singularities of the signal under study. All of the above shortcomings of the standard multifractal formalism introduce intrinsic insufficiencies in unraveling the true multifractal nature of rainfall fluctuations and may lead to misleading inferences. The methodology proposed herein does not suffer from the above shortcomings and has been documented in the turbulence literature (e.g., see [14,15]) to yield accurate and robust estimates of the multifractal spectra.

The innovations of the proposed methodology (which will become more apparent after the reader has read the theory behind the methodology presented in the next section; see also the review article of [18]) can be summarized as follows: (1) by using a wavelet-based formalism, wavelets of increasingly higher order can be easily employed to remove nonstationarities in the signal and define via analysis (as opposed to a priori specification) what are the rainfall "fluctuations" whose multifractal properties we seek to characterize; (2) by using wavelets of increasingly higher order we have access to the whole range of singularities as this range might not be known a priori (it is noted that by employing a structure function analysis, the maximum singularity exponent that can be detected is 1 and therefore we might bias the estimates of the intermittency coefficient and spectrum of singularities if singularities of Hölder exponent $h > 1$ end up being present in the signal); (3) by using the wavelet transform modulus maxima (WTMM), i.e., the maxima lines only instead of the whole continuous wavelet transform (CWT), a more efficient and robust estimate of the singularity spectrum can be obtained; (4) by using a cumulant analysis of the WTMM magnitudes [15], one can directly estimate from their behavior as a function of scale, the singularity spectrum $D(h)$; (5) the coefficients of the polynomial expansion of the scaling exponent function $\tau(q)$ can be directly computed and do not require taking higher order moments of the data.

In the next section, a brief review of the wavelet-based multifractal analysis is presented and references to the original publications are provided for proofs and details. Section 3 presents the results of applying the methodology to the analysis of three high resolution temporal rainfall series, each composed of 5 s sampling of rainfall intensity for several hours via an

optical raingauge. These series have been analyzed by others in the literature and provide a benchmark for comparison of methodologies and associated inferences. Finally conclusions and interpretations are given in Section 4.

2. Methodology overview

Let $f(x)$ be a function whose multifractal characteristics we wish to estimate. The local singularity of $f(x)$ at point x_0 is characterized by the Hölder exponent $h(x_0)$ defined as

$$\big|f(x) - P_n(x - x_0)\big| \leqslant C|x - x_0|^{h(x_0)}. \tag{1}$$

That is, $h(x_0)$ is the largest exponent such that there exists a polynomial $P_n(x)$ of degree n that satisfies the above condition in the neighborhood of x_0. (Note that $h(x_0)$ in (1) can be larger than 1, characterizing thus singularities in the higher order derivatives of the function, i.e., $n < h < n+1$ implies that the nth order derivative of $f(x)$ is singular.) Small values of $h(x_0)$ imply stronger singularities. The spectrum of Hölder exponents, or singularity spectrum $D(h)$, is defined as

$$D(h) = d_H\big(x, h(x) = h\big), \tag{2}$$

i.e., as the Hausdorff dimension d_H of the set of all points x such that $h(x) = h$.

The local singularity of $f(x)$ at point x_0 can be characterized by the behavior of the wavelet coefficients as they change with scale a (see [18]). Specifically, defining the continuous wavelet transform (CWT) of $f(x)$ using the analyzing wavelet ψ (e.g., [19,20]), as

$$T_\psi[f](b,a) = \frac{1}{|a|}\int f(x)\psi\left(\frac{x-b}{a}\right)dx, \quad a > 0,\ b \in R, \tag{3}$$

it can be shown that

$$T_\psi[f](x_0,a) = O\big(a^{h(x_0)}\big), \quad a \to 0, \tag{4}$$

provided that the order of the analyzing wavelet n_ψ (i.e., number of vanishing moments) is larger than the strength $h(x_0)$ of the singularity located at x_0. It is noted that to unravel all singularities in $f(x)$, n_ψ must be greater than the exponent of the weakest singularities present in the signal, i.e., $n_\psi > h_{\max}$. This is the reason that if the analyzing wavelet is chosen to have $n_\psi = 1$, i.e., similar to the structure function in a poor man's wavelet sense, no singularities $h > 1$ can ever be detected, biasing thus the estimate of $D(h)$ if singularities $h > 1$ are present in the signal [17]. Without knowing a priori what singularities are present in the signal, the approach we propose and use in this work is to use analyzing wavelets with $n_\psi = 1, 2, 3, \ldots$ and adopt that wavelet for which robust estimates of $D(h)$ are obtained. It is noted that this particular wavelet defines also the "fluctuations" of the process whose multifractal properties we seek to characterize. That is, the fluctuations superimposed on the underlying low-frequency component (filtered out via the wavelet) show scaling, while the background (low-frequency) itself does not.

By studying the behavior of only the maxima lines (see [18,21]), i.e., how the WTMM coefficients $|T_{\psi,\max}[f](x_0,a)|$ change as a function of scale, the structure of the singularities (the nonoscillating kind) in a signal can be more efficiently estimated than using the CWT. Specifically,

$$\big|T_a(x_0)\big| \sim a^{h(x_0)}, \quad a \to 0, \tag{5}$$

where $T_a(x_0)$ is an abbreviation for $T_{\psi,\max}[f](x_0,a)$. Eq. (5) implies that at any scale a, the statistical moments of the singularities $h(x)$, considered as random variables, can be obtained by the statistical moments of $\ln|T_a(x)|$. The classical WTMM method [18] actually amounts to computing the $D(h)$ singularity spectrum (Eq. (2)) via the estimate of the scaling behavior of the statistical moments of the WTMM coefficients:

$$N_a\big\langle\big|T_a(x)\big|^q\big\rangle \sim a^{\tau(q)}, \quad a \to 0, \tag{6}$$

where $N_a \sim a^{-D_f}$ is the number of maxima lines at scale a and $\langle . \rangle$ denotes the mean over x. A Legendre transform is applied to the $\tau(q)$ scaling exponents to get the $D(h)$ spectrum. The magnitude cumulant analysis [15] consists of noticing that Eq. (6) can be re-expressed in terms of the logarithm of the moment generating function (also called the cumulant function) of $\ln|T_a|$ at scale a:

$$\Psi_a(q) = \ln\big\langle e^{q\ln|T_a(x)|}\big\rangle = \sum_{n=1}^{+\infty} C_n(a)\frac{q^n}{n!}, \tag{7}$$

where the cumulants $C_n(a)$ of the WTMM magnitude can be obtained by taking the derivatives of $\Psi_a(q)$ at $q = 0$. By taking the logarithm of both sides of Eq. (6), and noticing that $\ln\langle|T_a(x)|^q\rangle$ is $\Psi_a(q)$, one obtains the following polynomial expansion for the scaling exponents spectrum $\tau(q)$:

$$\tau(q) = -D_f + \sum_{n=1}^{+\infty}(-1)^{n-1}c_n\frac{q^n}{n!} = -c_0 + c_1 q - c_2 q^2/2! + c_3 q^3/3! + \cdots, \quad (8)$$

where the c_n's are defined in terms of the cumulants $C_n(a)$ as

$$C_n(a) = (-1)^{n-1}c_n \ln a. \quad (9)$$

By comparing Eqs. (5) and (6), one can see that $\tau(q)$ relates to the cumulants of h. Specifically, the coefficients c_n in the $\tau(q)$ expansion of Eq. (8) are the coefficients that control the way the probability density function (PDF) of the random variable $h(x)$ shrinks to a delta distribution $\delta(h - c_1)$, where $c_1 = \langle h\rangle$, when $a \to 0$. Indeed, the cumulants of this PDF go to zero as $c_n/(\ln(1/a))^{n-1}$ for $n \geqslant 2$ (large deviations theory; see [22]). It is noted that the $D(h)$ singularity spectrum obtained by Legendre transforming the $\tau(q)$ curve provides an alternative geometrical point of view to this statistical formalism. As defined in Eq. (2), the $D(h)$ is maximum for $h = \langle h\rangle$ (see Fig. 1), which means that if $D_f = 1$, only the subset of points where the function is Hölder $h = \langle h\rangle$ will have finite Lebesgue measure; all the subsets corresponding to the other values of h between $h_{\min}$ and $h_{\max}$ will be Cantor-sets of zero length. Note that for a log-normal multifractal process, for which $D(h)$ is quadratic, all the c_n are zero for $n > 2$ [14,23]:

$$D(h) = c_0 - \frac{(h - c_1)^2}{2c_2}, \quad (10)$$

with $h_{\min,\max} = c_1 \mp \sqrt{2c_2 c_0}$.

In addition to the one-point WTMM statistics presented above, it is useful to study the two-point correlation function of $\ln|T_a(x)|$ [23], i.e.,

$$\mathcal{C}(a, \Delta x) = \big\langle\big(\ln|T_a(x)| - \langle\ln|T_a(x)|\rangle\big) \times \big(\ln|T_a(x + \Delta x)| - \langle\ln|T_a(x)|\rangle\big)\big\rangle. \quad (11)$$

By seeing how this two-point correlation changes as a function of Δx at scale a, one can determine the nature of the correlations in the signal. For example, if $\mathcal{C}(a, \Delta x)$ is logarithmic in Δx and independent of scale a provided that $\Delta x > a$, i.e.,

$$\mathcal{C}(a, \Delta x) \sim \ln \Delta x, \quad \Delta x > a, \quad (12)$$

then long-range dependence is inferred. Moreover, [23,24] have shown that for random multiplicative cascades on wavelet dyadic trees (see also [25])

$$\mathcal{C}(a, \Delta x) \sim -c_2 \ln \Delta x, \quad (13)$$

where the proportionality coefficient c_2 is the same as the proportionality coefficient of $C_2(a)$ versus $\ln(a)$, defined in Eq. (9), i.e.,

$$\mathcal{C}(a, \Delta x = 0) \equiv C_2(a) \sim -c_2 \ln a. \quad (14)$$

By computing $\mathcal{C}(a, \Delta x)$ from Eq. (11) and plotting it as a function of $\ln \Delta x$, inferences can be made about long-range dependence and consistency with a multiplicative cascading process. Note that the presence of multifractality does not necessarily imply either long-range dependence or multiplicative cascade [14]. In making inference from data, it is often helpful to superimpose on the same plot the curves $\mathcal{C}(a, \Delta x)$ vs. $\ln \Delta x$ for several $\Delta x > a$ and the $C_2(a)$ vs. $\ln a$ curve and see whether their slopes agree as a consistent estimate of the intermittency coefficient c_2.

Before the application of the above methodology to the high-resolution rainfall intensity series is presented in the next section, an important additional technicality is discussed. As has been shown in [18], low values of the WTMM coefficients can result in divergence and numerical instabilities of Eq. (6), especially for $q < 0$, and thus unreliable estimates of the $\tau(q)$ and $D(h)$ curves. To alleviate this problem, the previous authors proposed to replace the value of the wavelet transform modulus at each maximum by the supremum value along the corresponding maxima line at scales smaller than a. This method referred to as "WTMM with sup" has been used in our analysis as divergence problems were encountered for negative moments. There is an important technicality that results when using the "WTMM with sup" method: it cannot identify singularities $h < 0$. This can be understood by noting that if there is any singularity with $h < 0$, the modulus of the wavelet transform of the signal would not decay but rather increases from large to small scales. Thus, if one were to replace the modu-

lus maxima with *sup* along a maxima line, that would result in an horizontal maxima line and thus a trivial incorrect value of zero for h. Since we do not know a priori whether any negative singularities might be present in rainfall, we use the following simple trick. Instead of working with rainfall intensities themselves, we work with the cumulative of the rainfall intensities (i.e., the integral of the signal). Thus any singularities $-1 < h < 0$ in the original signal will become singularities of order $0 < h < 1$ in the cumulative rainfall allowing thus to use the numerically preferred "WTMM with sup" methodology. Once the $D(h)$ curve of the cumulative rainfall is estimated, it is shifted by one to the left, i.e., $D^I(h) = D^c(h+1)$ (the superscripts I and c refer to intensities and cumulative rain, respectively) and inferences are made for rainfall intensities themselves. The reader is referred to several original publications for the wavelet-based multifractal analysis formalism ([14,15,17,23]), and especially the review article of [18] and [24,26] for details and proofs.

3. Analysis of rainfall data

Three rainfall intensity time series over Iowa City, sampled every 5 s, have been used in this analysis (see [4] for data collection details and also [6] for scaling and multifractal analysis of these same series). We will refer to these series as Rain 6 (3 May 1990; 6661 samples); Rain 5 (1 November 1990; 6689 samples) and Rain 4 (3 October 1990; 6689 samples) to be consistent with the original nomenclature. Fig. 2 shows a plot of these series.

For the reasons explained in the previous section, the "WTMM with sup" method has been applied to the cumulative of the rainfall intensities. Wavelets with varying number of vanishing moments, $n_\psi = 1, 2, 3$ and 4, referred to as $g^{(n_\psi)}$, have been used. More precisely $g^{(n_\psi)}$ corresponds to the n_ψ-th derivative of the Gaussian function. Note that $g^{(1)}$ and $g^{(2)}$ on the cumulative rainfall are analogous to $g^{(0)}$ (box-counting) and $g^{(1)}$ (structure function), respectively, on the rainfall intensities. Fig. 3 shows the cumulative of Rain 6,

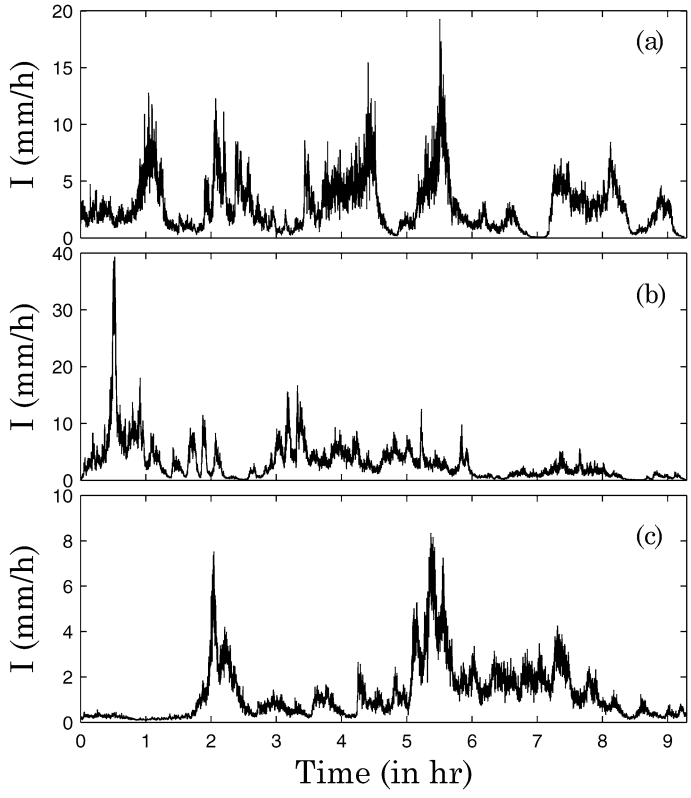

Fig. 2. Time series of rainfall intensity (mm/h) for Rain 6 (a), Rain 5 (b) and Rain 4 (c) (see text for details).

S0375-9601(05)01325-3/SCO AID:14863 Vol.●●●(●●●)
PLA:m3 v 1.46 Prn:13/09/2005; 8:26
pla14863
[DTD5] P.6 (1-11)
by:PS p. 6

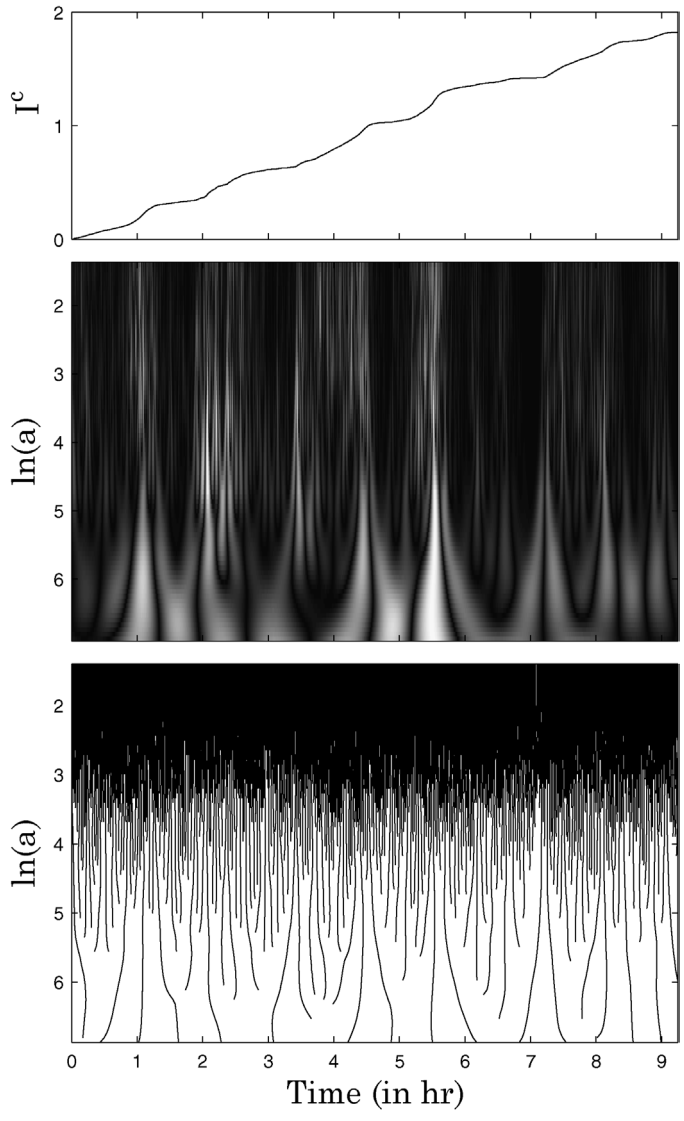

Fig. 3. (Top) Cumulative rainfall (Rain 6) (in 10^4 mm/h) versus time (h). (Middle) Time-scale wavelet transform representation of cumulative rainfall with the analyzing wavelet $g^{(3)}$. The modulus of the wavelet transform is coded, independently at each scale a, using 64 grey levels from black ($|T_{g^{(3)}}(t,a)| = 0$) to white ($\max_t |T_{g^{(3)}}(t,a)|$). (Bottom) Wavelet transform skeleton defined by the maxima lines. The scale a is expressed in sampling time ($\Delta t = 5$ s) unit.

its continuous wavelet transform and the corresponding wavelet transform skeleton defined by the maxima lines, when analyzed using $g^{(3)}$. The cumulants $C_n(a)$ have been computed, and are shown in Fig. 4 vs. $\ln a$. ($C_0(a) = -c_0 \ln a$ is evaluated as the logarithm of the number of maxima lines N_a at each scale a.) The following observations can be made from these plots:

- $C_0(a)$ vs. $\ln a$ (Fig. 4(a)) has a slope of approximately -1 (i.e., $c_0 = 1$), implying that singularities are present throughout the signal, i.e., the fractal dimension of the support of singularities is $D_f = 1$.
- $C_1(a)$ vs. $\ln a$ (Fig. 4(b)) shows that using $g^{(1)}$, we get a slope of 1. It is important to note that this slope (corresponding to a box counting method on the rainfall intensities) is an erroneous/trivial estimate,

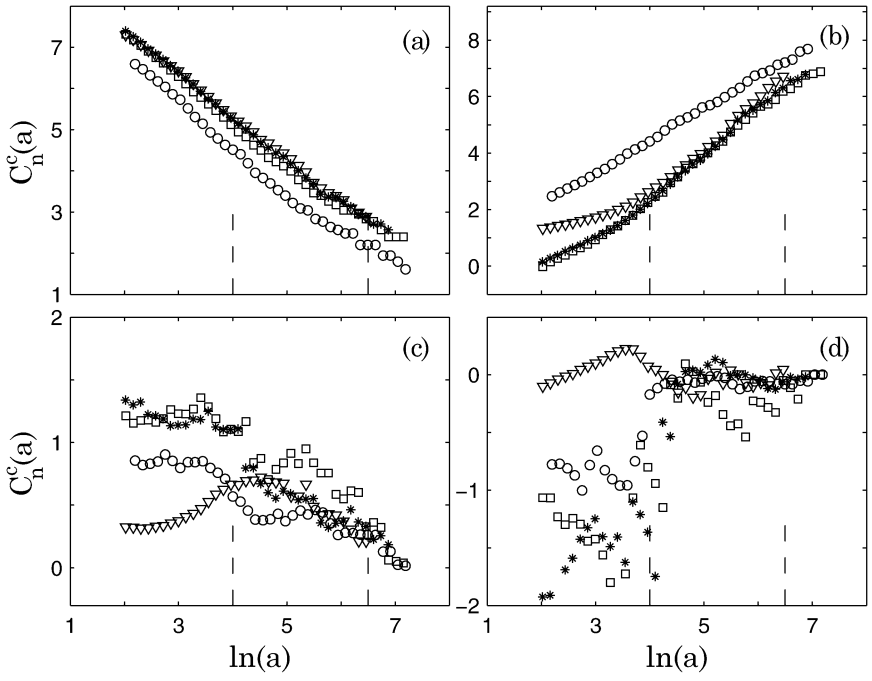

Fig. 4. Cumulant analysis of the cumulative rainfall (Rain 6) using the WTMM method with the analyzing wavelets $g^{(1)}$ (○), $g^{(2)}$ (□), $g^{(3)}$ (∗) and $g^{(4)}$ (▽). $C_n^c(a)$ versus $\ln(a)$ for $n = 0$ (a), 1 (b), 2 (c) and 3 (d). The vertical dashed lines delimit the range of scales (expressed in 5 s unit) used for the linear regression estimate of c_n^c.

since $C_1(a)$ vs. $\ln a$ using higher order wavelets, yields a slope larger than 1. The results become robust with $g^{(3)}$ and $g^{(4)}$, thus establishing that the appropriate wavelet for the cumulative rain is $g^{(3)}$ (and thus $g^{(2)}$ for rainfall intensities themselves).

- Scaling of $C_1(a)$ (Fig. 4(b)), $C_2(a)$ (Fig. 4(c)), and $C_3(a)$ (Fig. 4(d)) vs. $\ln a$ is observed only within the scales of $\ln a = 4$ to approximately $\ln a = 6.5$, corresponding to a range of scales of 4 min to 1 hour.
- Fitting straight lines in the plots of Fig. 4 results in the c_n coefficients ($n = 0, 1, 2, 3$) for all 4 wavelets, as shown in Table 1.

Table 1
Estimates of c_n^c for the cumulative rainfall (Rain 6) obtained from cumulant analysis using the WTMM method over the range of scales 4–58 min (the error bars were obtained from the standard deviation of the local slope fluctuations)

	c_0^c	c_1^c	c_2^c	c_3^c
$g^{(1)}$	0.94 ± 0.05	1.11 ± 0.02	0.15 ± 0.02	~ 0
$g^{(2)}$	0.95 ± 0.04	1.54 ± 0.03	0.28 ± 0.05	~ 0
$g^{(3)}$	0.98 ± 0.02	1.64 ± 0.03	0.26 ± 0.04	~ 0
$g^{(4)}$	1.00 ± 0.02	1.69 ± 0.06	0.24 ± 0.05	~ 0

The conclusion from this analysis is that rainfall fluctuations (defined as the convolution of the original rainfall intensity series with a Gaussian wavelet with 2 vanishing moments) exhibit multifractality between the scales of 4–5 min to 1 hour, with cumulant coefficients: $c_0^I = c_0^c = 0.98 \pm 0.02$; $c_1^I = c_1^c - 1 = 0.64 \pm 0.03$; $c_2^I = c_2^c = 0.26 \pm 0.04$ and $c_3^I = c_3^c \sim 0$ (obtained from the values of Table 1 with $g^{(3)}$ on the cumulative rainfall, and having moved $D(h)$ to the left by 1 along the h axis, which affects only the value of c_1).

Assuming that $c_3^c = 0$ (there is no way to claim that $c_3^c \neq 0$ from the small data set under study), and using the values of c_0^c, c_1^c and c_2^c obtained from analyzing the cumulative rainfall series using $g^{(3)}$, we compute the spectrum of scaling exponents $\tau^c(q)$ using Eq. (8), and the spectrum of singularities $D(h)$ using Eq. (10). The corresponding curves for $\tau^I(q) = \tau^c(q) - q$ and $D^I(h) = D^c(h + 1)$ are shown in Fig. 5. On the same

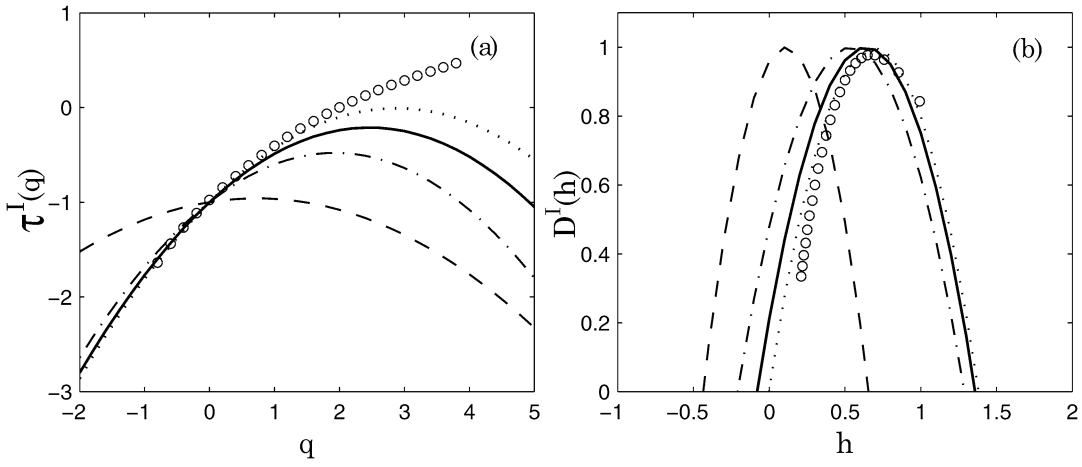

Fig. 5. $\tau^I(q)$ $(=\tau^c(q)-q)$ spectrum and (b) $D^I(h)$ $(=D^c(h+1))$ singularity spectrum for rainfall intensity fluctuations of Rain 6. These spectra were obtained for the cumulative rainfall using cumulant analysis with wavelets $g^{(1)}$ (dashed), $g^{(2)}$ (dotted dashed), $g^{(3)}$ (solid) and $g^{(4)}$ (dotted). The symbols (○) correspond to the spectra obtained using the (moment) WTMM method with $g^{(3)}$.

Table 2
Estimates of c_n^I for rainfall intensity obtained from the cumulant analysis of the cumulative rainfall data Rain 6, Rain 5, and Rain 4 using the WTMM method with $g^{(3)}$ over the range of scales 4–58 min

	c_0^I	c_1^I	c_2^I	c_3^I
Rain 6	0.98 ± 0.02	0.64 ± 0.03	0.26 ± 0.04	~ 0
Rain 5	0.97 ± 0.02	0.55 ± 0.05	0.38 ± 0.05	~ 0
Rain 4	0.99 ± 0.02	0.62 ± 0.03	0.35 ± 0.15	~ 0

plots, we also show the $\tau^I(q)$ and $D^I(h)$ curves obtained when using $g^{(1)}$, $g^{(2)}$ and $g^{(4)}$ on the cumulative rain. It is seen again that $g^{(1)}$ (i.e., box-counting on the intensities) would give misleading results. For comparison, we show in Fig. 5 (circles) the $\tau^I(q)$ curve obtained by a moment analysis (not cumulant analysis) using $g^{(3)}$ (i.e., $g^{(2)}$ on the intensities). The deviation of the moments vs. cumulant results for $q > 2-3$ might be due to either (a) assumption of $c_3^I = 0$ in the cumulant analysis, while in fact it is not; or (b) a lack of statistical convergence of the higher order moments in the moment analysis owing to small sample size. The same analysis was applied to Rain 5 and Rain 4 and the plots of $C_n^c(a)$ vs. $\ln(a)$ (not shown here) displayed linearity over the same range of scales. The estimated c_n^I coefficients for all three series are shown in Table 2. It is observed that the estimates are robust: $c_0^I \simeq 1.0$, $c_1^I = 0.55 - 0.64$, $c_2^I = 0.26 - 0.38$ and $c_3 \sim 0$, although Rain 5 and Rain 4 look slightly more intermittent than Rain 6, a result that might not be statistically significant.

The two-point WTMM magnitude correlation analysis for Rain 6 and Rain 5 is shown in Fig. 6 using the CWT with $g^{(2)}$ directly on rainfall intensities (left plot), and the "WTMM with sup" and $g^{(3)}$ on the cumulative rain (right plot). The solid curves are lines obtained for different scales a chosen in the scaling range evidenced in Fig. 4. The fact that for $\Delta t > a$, all the curves fall on the top of each other and are almost linear is a strong indication that Eq. (12) holds implying a long-range dependence in rainfall fluctuations. The slopes of these lines are very close to $-c_2$ up to numerical uncertainty (see solid straight line plotted for $c_2 = 0.26$ for Rain 6 and $c_2 = 0.38$ for Rain 5 and also compare with the $C_2(a)$ vs $\ln a$ curve (circles) displayed on the same plots), implying that the long-range dependence found in the series is consistent with both Eqs. (13) and (14) and therefore is likely to be the signature of the existence of an underlying multiplicative cascade process. Note that, as seen in Fig. 6(a) and (b), the statistics of the CWT coefficients are nearly Gaussian ($C_2^I(a) = \pi^2/8$) at a scale $a \sim 1$ hour that coincides with the time lag beyond which the WTMM magnitudes become decorrelated ($\mathcal{C}(a, \Delta t) \simeq 0$) and which evidently corresponds to the characteristic storm pulse duration.

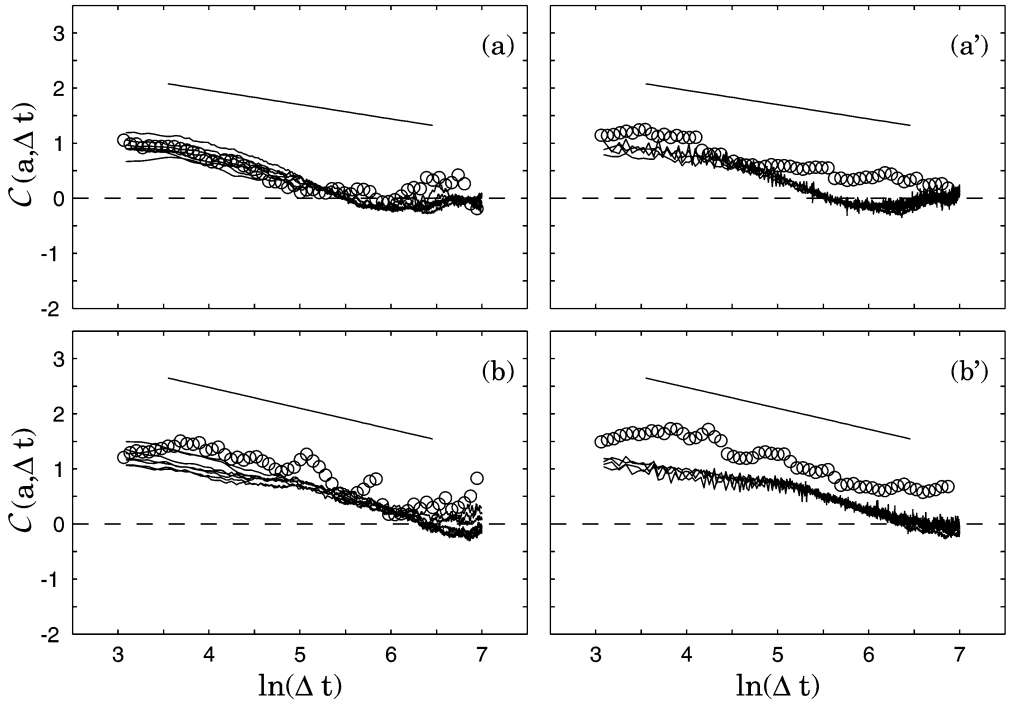

Fig. 6. Two point magnitude correlation functions $\mathcal{C}(a, \Delta t)$ versus $\ln(\Delta t)$ for rainfall intensity using the CWT method with $g^{(2)}$ (left column) and for cumulative rainfall using WTMM with $g^{(3)}$ (right column). From top to bottom: Rain 6 (a), (a'), Rain 5 (b), (b'). For comparison is shown the behavior of the corresponding second order cumulant $C_2^I(a)$ (left column) and $C_2^c(a)$ (right column) versus $\ln(a)$, plotted as open circles. Note that for the CWT estimate of $C_2^I(a)$, we have actually plotted $C_2^I(a) - \pi^2/8$ to evidence that the statistics of CWT is nearly Gaussian ($C_2^I(a) - \pi^2/8 = 0$) at the scale of the duration of the storm which also corresponds to the decorrelation length where $\mathcal{C}(a, \Delta t) = 0$. In each panel, the solid line corresponds to the estimated slope $-c_2$ of the corresponding second order cumulant (see Table 2).

Although no direct comparison can be made between our study, and that of [6] whose purpose was modeling, we note that both studies agree in inferring a multiplicative structure of the underlying rainfall mechanism. While we identify a scaling regime of rainfall fluctuations (properly defined by removing nonstationarities) between the scales of 4 min and 1–2 hours, Veneziano et al. identify four spectral regimes between the scales of a few seconds to several hours (a segmented spectrum) and deal with nonstationarities by proposing a stationary model for the central part of the storm, and a nonstationary model for the build-up and decay phases. We believe that the difference in the scaling range inferences stems from the wavelet-based methodology proposed here, which is a comprehensive framework that allows us to (i) account for nonstationarities appropriately, and (ii) analyze the whole signal at once, and therefore more accurately identify the scaling range present in the signal.

4. Conclusions

In this work, a wavelet-based multifractal formalism was applied for the first time to high resolution temporal rainfall series. The advantages and versatility of this methodology compared to traditional moment-based analysis (e.g., box-counting or structure function analysis) were discussed. The main findings can be summarized as follows:

- Rainfall intensity fluctuations were found to exhibit multifractality between the scales of 4–5 min and 1–2 hours, which coincides with the duration of storm pulses for the events under study. Between the scales of 5 s and 5 min, a different regime was found which needs further investigation. Above the storm pulse duration, no scaling could be identified with our small data sets.

• Rainfall intensity fluctuations were found to exhibit a wide spectrum of singularities with the possible presence of (i) $h < 0$ implying that there are regions (Cantor set of points) in the rainfall signal at which the process is not continuous and (ii) $h > 1$ implying that there are regions at which the process is likely to be continuous and once differentiable. Within the log-normal approximation of the $D(h)$ singularity spectrum (Eq. (10)), the results in Table 2 yield $h_{\min} = c_1 - \sqrt{2c_2c_0} \simeq -0.1$ and $h_{\max} = c_1 + \sqrt{2c_2c_0} \simeq 1.3$.

• For rainfall fluctuations, we found that $c_1 = \langle h \rangle \simeq 2/3$ implying that they are smoother on the average than velocity fluctuations in turbulent flows (for which $c_1 = \langle h \rangle \simeq 1/3$). Also we found that the intermittency coefficient $c_2 \simeq 0.3$, which is an order of magnitude larger than that found for turbulent velocity fluctuations ($c_2 \simeq 0.025$ and 0.04 respectively for longitudinal and transverse velocity increments; see [22]) implying a significantly larger variability of singularities at any scale.

• Rainfall fluctuations were found to have a long-range dependence up to the scale of the storm pulse duration, and this dependence was found consistent with that of a multiplicative cascade process. This is interpreted as the possibility of a multiplicative cascading mechanism giving rise to storm rainfall which however is local, i.e., within storm pulses, and does not hold from one storm pulse to another.

• The intermittency coefficient of $c_2 \approx 0.3$ is of the same order of magnitude as found for enstrophy ($c_2 \approx 0.3$) and energy dissipation ($c_2 \approx 0.2$) in fully developed turbulence (see [22,27]). The interpretation of this is not clear and needs further investigation.

A word of caution is in order. It is noted that the record length is very small (≈ 6000 points) and within each storm approximately 1000 points. This makes it difficult to get robust estimates of the multifractal properties and is the main reason that we have carefully used all possible methods (CWT, WTMM and WTMM with sup, and with wavelets of different orders) to get reliable estimates. Although it is encouraging that the results from all three storms point to the same conclusions (see also a much more elaborate analysis of these and an additional storm in [28]), further analysis of other storms and longer records should be pursued such that (i) the local (within storm-pulse) multifractality and cascading mechanism can be more definitely confirmed, and (ii) the inter storm-pulse statistical distribution can be investigated.

Acknowledgements

This work was partially supported by NSF (grant ATM-0130394) and NASA (grant NAG5-12909 and NAG5-13639) to EFG. The data were collected at the Hydro-Meteorology Lab of the Iowa Institute of Hydraulic Research, under the supervision of Konstantine Georgakakos. We thank Anton Kruger for his help with the data. Computational resources were provided by the Minnesota Supercomputing Institute, Digital Technology Center, at the University of Minnesota.

References

[1] D. Schertzer, S. Lovejoy, J. Geophys. Res. 92 (1987) 9693.
[2] S. Lovejoy, D. Schertzer, Multifractal analysis techniques and the rain and cloud fields from 10^{-3} to 10^{6}, in: D. Schertzer, S. Lovejoy (Eds.), Non-Linear Variability in Geophysics: Scaling and Fractals, Kluwer Academic, Norwell, MA, 1991.
[3] J. Olsson, J. Niemczynowicz, R. Berndtsson, J. Geophys. Res. 98 (D12) (1993) 23265.
[4] K.P. Georgakakos, A.A. Cârsteanu, P.L. Sturdevant, J.A. Cramer, J. Appl. Meteorol. 33 (12) (1994) 1433.
[5] D. Marsan, D. Schertzer, S. Lovejoy, J. Geophys. Res. 101 (D21) (1996) 26333.
[6] D. Veneziano, R.L. Bras, J.D. Niemann, J. Geophys. Res. 101 (D21) (1996) 26371.
[7] A. Cârsteanu, E. Foufoula-Georgiou, J. Geophys. Res. 101 (D21) (1996) 26363.
[8] Venugopal V., E. Foufoula-Georgiou, J. Hydrol. 187 (1996) 3.
[9] D. Harris, M. Menabde, A. Seed, G. Austin, Nonlinear Proc. Geophys. 5 (1998) 93.
[10] R. Deidda, R. Benzi, F. Siccardi, Water Resour. Res. 35 (1999) 1853.
[11] M. Menabde, M. Sivapalan, Water Resour. Res. 36 (11) (2000) 3293.
[12] D. Veneziano, V. Iacobellis, Water Resour. Res. 38 (8) (2002) 1138, 10.1029/2001WR000522.
[13] L. Ferraris, V. Gabellani, V. Parodi, N. Rebora, J. von Hardenberg, A. Provenzale, J. Hydrometeorol. 4 (2003) 544.
[14] A. Arneodo, S. Manneville, J.F. Muzy, S. Roux, Philos. Trans. R. Soc. London A 357 (1999) 2415.
[15] J. Delour, J.F. Muzy, A. Arneodo, Eur. Phys. J. B 23 (2001) 243.
[16] A. Davis, A. Marshak, W. Wiscombe, Wavelet-based multifractal analysis of non-stationary and/or intermittent geophysical signals, in: E. Foufoula-Georgiou, P. Kumar (Eds.), Wavelets in Geophysics, Academic Press, San Diego, CA, 1994.

S0375-9601(05)01325-3/SCO AID:14863 Vol.●●●(●●●)
PLA:m3 v 1.46 Prn:13/09/2005; 8:26

[17] J.F. Muzy, E. Bacry, A. Arneodo, Phys. Rev. E 47 (2) (1993) 875.
[18] J.F. Muzy, E. Bacry, A. Arneodo, Int. J. Bifur. Chaos 4 (2) (1994) 245.
[19] I. Daubechies, Ten Lectures on Wavelets, CBMS-NSF Reg. Conf. Ser. Appl. Math., vol. 61, SIAM, Philadelphia, PA, 1992.
[20] S. Mallat, A Wavelet Tour in Signal Processing, Academic Press, New York, 1998.
[21] S. Mallat, W.L. Hwang, IEEE Trans. Inf. Theory 38 (1992) 617.
[22] U. Frisch, Turbulence, Cambridge Univ. Press, Cambridge, 1995.
[23] A. Arneodo, E. Bacry, S. Manneville, J.F. Muzy, Phys. Rev. Lett. 80 (1998) 708.
[24] A. Arneodo, E. Bacry, J.F. Muzy, J. Math. Phys. 39 (1998) 4142.
[25] J. O'Neil, C. Meneveau, Phys. Fluids A 5 (1993) 158.
[26] E. Bacry, J.F. Muzy, A. Arneodo, J. Stat. Phys. 70 (1993) 635.
[27] P. Kestener, A. Arneodo, Phys. Rev. Lett. 91 (2003) 194501.
[28] Venugopal V., S.G. Roux, E. Foufoula-Georgiou, A. Arneodo, Revisiting multifractality of high resolution temporal rainfall using a wavelet-based formalism, Water Resour. Res. (2005), submitted for publication.